

Unidirectional pinning in irradiated $\text{Bi}_2\text{Sr}_2\text{CaCu}_2\text{O}_8$ (invited)

L. Klein, E. R. Yacoby, A. Tsameret, and Y. Yeshurun
Department of Physics, Bar-Ilan University, 52900 Ramat-Gan, Israel

K. Kishio
Department of Industrial Chemistry, University of Tokyo, Bunkyo-ku, Tokyo 113 Japan

$\text{Bi}_2\text{Sr}_2\text{CaCu}_2\text{O}_8$ crystals were irradiated with heavy ions (Pb, Xe) to produce columnar defects along the c direction or at 45° with respect to it. We describe the dependence of the critical currents, irreversibility fields, pinning force, and magnetic relaxation rates on the dose and on the type of ions. The irreversible properties of the Pb-irradiated samples are more enhanced than those of the Xe-irradiated sample at low temperatures, and vice versa at high temperatures. At low temperatures the efficiency of the columnar defects is enhanced with the ion dose but, at high temperatures, the maximum dose (2.5×10^{11} ions/cm²) is less efficient than intermediate doses. The unidirectional nature of the columnar pinning centers serves to demonstrate that the vortices maintain linelike features. For most of the irradiated samples, the pinning force density data are reduced to a single curve below 45 K. The relaxation rates at low temperatures reflect thermal reduction of the effective pinning barriers.

I. INTRODUCTION

$\text{Bi}_2\text{Sr}_2\text{CaCu}_2\text{O}_8$ (BSCCO) is characterized by weak flux pinning even relative to other high-temperature superconductors (HTS). This is reflected in its low critical currents and low irreversibility fields,¹ which hinder high-current applications. Therefore, the possibility of enhancing the pinning force is important not only for studying the flux properties, but also as an indication of the possibility of reaching critical currents that will enable high-current applications. BSCCO is also one of the most anisotropic compounds among the known cuprate HTS, due to the weak coupling between the Cu-O layers. The effect of the coupling on the vortex properties is still debated. In particular, it is still unclear in what range of field and temperature the coupling is important and the vortices are linelike, and at what range the coupling can be neglected and the vortices are two dimensional "pancakes".² References 3–15 list some of the experimental works dealing with this issue.

Columnar defects are now a common probe for studying flux properties in HTS.^{12–20} These defects, induced by heavy-ion irradiation, have several advantages. Columnar defects are very efficient pinning centers; thus their effect indicates how much the pinning force may be artificially enhanced. In addition, these defects are oriented and it is possible to distinguish between linelike vortices and pure two-dimensional pancakes by looking for the dependence of pinning properties on the angle between the applied field and the defects.^{13–15} Linelike vortices are most efficiently pinned when they are oriented along the defect, and tilting them away from the defects should decrease pinning. On the other hand, no angular dependence is expected for two-dimensional pancakes, since the density of pinning centers in each Cu-O plane is what matters, and the correlation of pin-

ning centers at different planes is not relevant. Thus, important information concerning the vortices dimensionally may be obtained by studying the angular dependence of the pinning properties.^{13–15}

In previous works^{13–15} we have demonstrated the unidirectional nature of the columnar defects in BSCCO via the hysteresis loops, $M(H)$. Typical results are shown in Fig. 1. The figure describes the evolution of the unidirectional pinning with temperature via the difference between the hysteresis loops recorded for field in the direction of the columnar defect ($+45^\circ$) and for the field perpendicular to it (-45°) for sample B3 (see Table I). We find that the magnetization is largest for fields applied along the defects and conclude that this unidirectional pinning indicates the linelike nature of

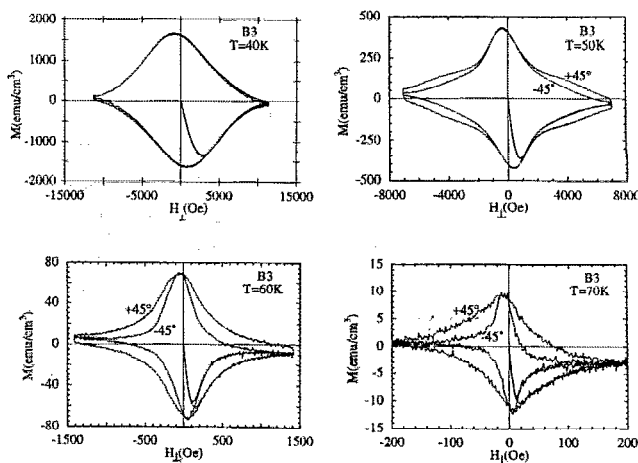


FIG. 1. Magnetization curves for sample B3 with the applied field at $\pm 45^\circ$ relative to the c direction at 40, 50, 60, and 70 K.

TABLE I. Information on the samples under investigation. Dimensions, ion type, dose, angle of irradiation, and the effective pinning at $T = 20$ K.

	Dimensions (mm ³)	Ion	Dose (ions/cm ²)	ϕ (deg)	U_{eff} (eV) $T = 20$ K
B0	1.25×0.75×0.05	---	---	---	0.0065
B1	1.5×1.1×0.044	Pb	10 ¹⁰	0	0.049
B2	1.6×0.95×0.046	Pb	10 ¹¹	0	0.045
B3	1.6×0.9×0.046	Pb	10 ¹¹	45	0.056
B4	1×0.95×0.042	Pb	2.5×10 ¹¹	0	0.055
B5	1.3×0.66×0.0835	Xe	10 ¹¹	45	---

vortices in BSCCO. In this article we pursue these previous works and describe extensive magnetic measurements on BSCCO crystals irradiated with Pb or with Xe ions. We report on (i) the dependence of the critical current and (ii) the dependence of the irreversibility line on the dose and on the type of irradiation; (iii) the scaling properties of the pinning force density; (iv) the angular dependence of J_c and the irreversibility line; and (v) a preliminary study of relaxation of the remanent magnetization.

II. EXPERIMENT

The measurements were performed on BSCCO crystals irradiated with 5.8-GeV Pb ions or 6-GeV Xe ions along the c direction or at 45° with respect to it. Irradiation was carried out at the Grand Accélérateur National d'Ions Lourds (GANIL, Caen, France). The Pb ions produce *continuous* columnar defects along their paths. The Xe ions did not produce columnar defects, but only clouds of clusters dispersed around the ion trajectory. In the case where the diameter of these clouds is smaller than the distance between two neighboring ion trajectories, the Xe ions tracks act as correlated disordered defects.²¹ All our measurements were performed on an Oxford Instruments vibrating sample magnetometer (VSM). The sample preparation is described in Ref. 22. The transition temperature $T_c = 85$ K of the unirradiated samples is reduced by less than 0.5 K after irradiation. Table I lists the samples under investigation, their dimensions, and the details of ion irradiation.

III. RESULTS AND DISCUSSION

A. Critical currents

The critical currents were estimated from the width of the magnetization curves, using the Bean model²³ for rectangular samples.²⁴ The main response of the sample magnetization is in the Cu-O planes, i.e., the response due to H_{\perp} (the component of the field perpendicular to the planes). Therefore, in comparing magnetization curves with the applied field at different angles relative to the c direction, we use H_{\perp} values. Figure 2(a) shows the critical current J_c as a function of temperature, at a constant field $H_{\perp} = 0.75$ T, applied along the defect, for the BSCCO crystal under investigation. Note that H_{\perp} is larger than the self-field²⁵ $H_s \approx J_c d$ (d is the shortest dimension of the sample), in order to avoid uncertainties in determination of J_c . The figure shows that (I) the critical current increases with the dose and (II) the Pb irra-

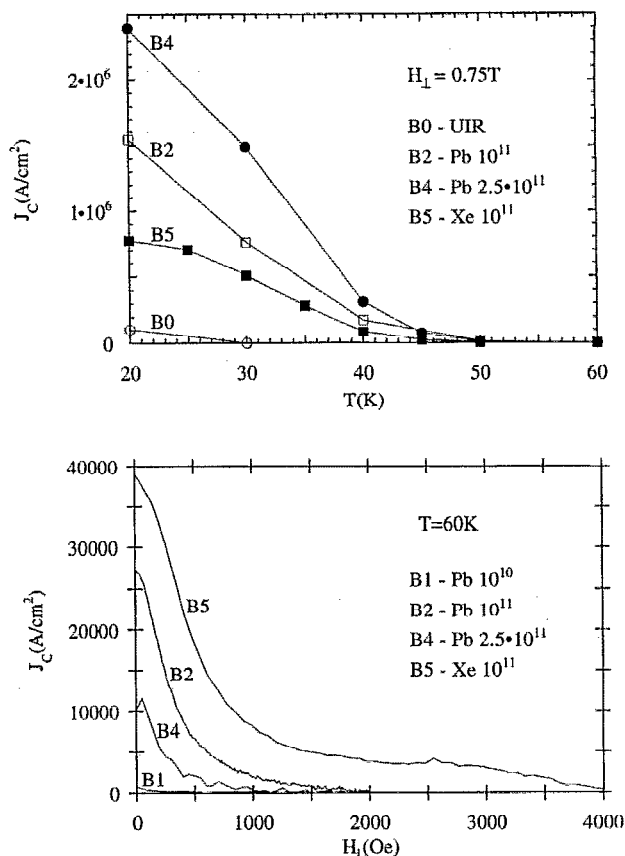


FIG. 2. (a) The critical current density as a function of temperature at $H_{\perp} = 0.75$ T for various samples. (b) The critical current density at $T = 60$ K as a function of magnetic field for the irradiated samples.

diation is more efficient in enhancing J_c than the Xe irradiation. As we show below, these two observations hold only below 50 K.

Figure 2(b) shows the critical current as a function of field, for the isotherm $T = 60$ K, for irradiated BSCCO crystals. We note that H_s at 60 K in these samples is not larger than 300 Oe. At this temperature, J_c of sample B4 (Pb-irradiated, 2.5×10^{11} ions/cm²) is smaller than that of B2 (Pb, 10^{11}). Also, it is apparent that the critical current of sample B5 (Xe-irradiated, 10^{11}) is higher than the critical current of all other irradiated samples. Thus, at approximately 50 K there are two crossover phenomena: first, in the efficiency of the columnar defect, the maximum dose becomes relatively less efficient at high temperatures; second, in the efficiency of the defects created by the Xe irradiation: at low temperatures, columns produced by Pb ions are more efficient in flux trapping than defects produced by Xe ions, whereas at high temperatures the reverse situation is observed. Insight into these phenomena is obtained from the analysis of the irreversibility line and the pinning force density, which follows below.

B. Irreversibility line (IRL)

The irreversibility field was determined from the hysteresis loops with a criterion of $J_c < 100$ A/cm². Figure 3 shows the irreversibility field as a function of temperature for different doses and types of irradiation. Note that in this figure

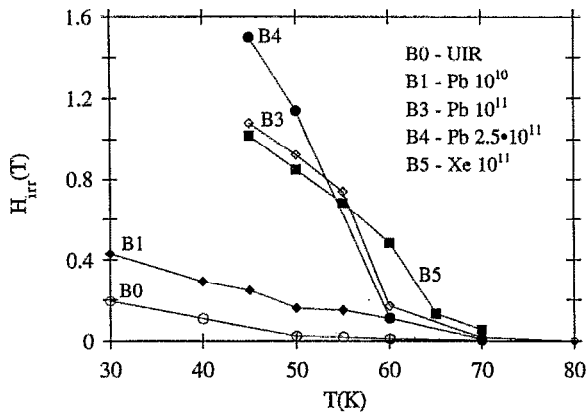


FIG. 3. The irreversible field H_{irr} as a function of temperature for various samples.

we present the IRL of sample B3; the IRL of sample B2 (the same dose but irradiated in the c direction) is almost the same. The irradiation shifts the irreversibility field upwards in a significant way. At low temperatures, the shift is more pronounced for higher doses of irradiation. However, at temperatures above 55 K this is not the case. Between 50 and 60 K there is a crossing of the irreversibility lines of the samples irradiated by Pb ions with doses of 10^{11} and 2.5×10^{11} ions/cm² (samples B3 and B4, respectively). This crossover indicates that there is an optimum irradiation dose of Pb ions at high temperatures above which the critical current becomes smaller.

The crossover can probably be related to a transition between two mechanisms of nonlogarithmic creep processes. It was theoretically shown²⁶ that a creep process in the presence of columnar defects is governed by a nucleation motion of vortex lines. Such a motion can be realized by two different mechanisms. At a low density of columnar defects, when the transverse localization length of a vortex line L_{\perp} is smaller than d_r , the averaged distance between the columnar defects, the creep process is dominated by the motion of vortex lines to the bulk after being liberated from the columnar defect. At high density of columnar defects, when L_{\perp} is comparable with d_r , the creep process is dominated by a motion of flux lines via a sequence of hops from one columnar defect to an adjacent one. The increase of columnar defects density results therefore in a suppression of the effective barrier for flux creep and in the enhancement of the relaxation rate. The crossover temperature between the two processes depends on the density of defects and occurs at lower temperatures for the larger dose. This crossover in the flux-creep process, which was identified experimentally²⁷ in BSCCO crystals with columnar defects, is probably responsible for the crossovers of J_c and of the IRLs between samples B3 and B4.

Another interesting feature apparent from Fig. 3 is the crossing of the IRLs of the Xe-irradiated sample (B5) and those of the Pb-irradiated samples (B3 and B4) at 55 K. At low temperatures the IRL of the Xe-irradiated sample (B5) follows the IRL of the sample irradiated by Pb ions with the same dose (10^{11} , B3). At 55 K, however, the IRLs of the

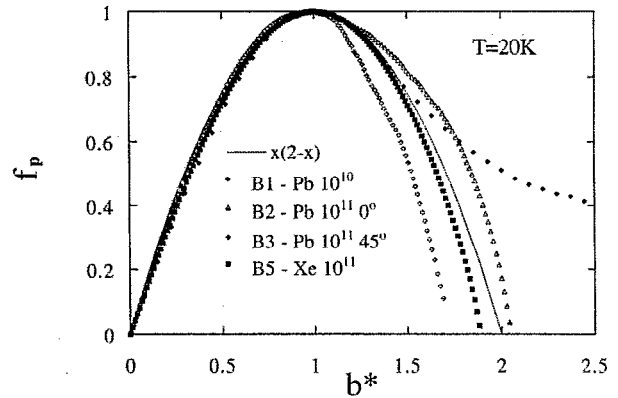
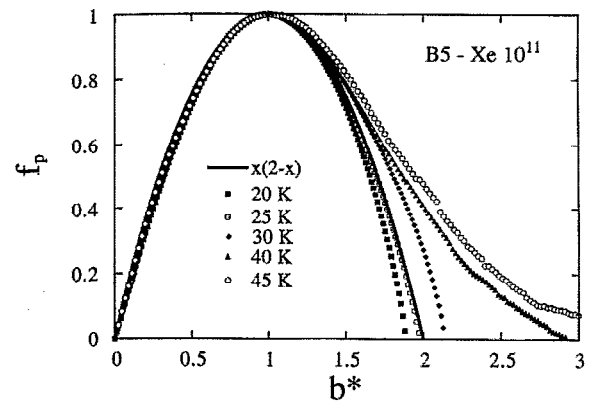


FIG. 4. (a) The rescaled pinning force density $f_p = F_p/F_{p,max}$ as a function of the reduced field $b^* = H/H_{max}$, for sample B5 at various temperatures. The solid line denotes the function $b^*(2-b^*)$. (b) The rescaled pinning force density $f_p = F_p/F_{p,max}$ as a function of the reduced field $b^* = H/H_{max}$, for various irradiated samples at $T=20$ K. The solid line denotes the function $b^*(2-b^*)$.

Pb-irradiated samples decrease rapidly whereas the IRLs of the Xe-irradiated sample decrease quite slowly with T . This indicates that the efficiency of columnar defects produced by the Pb ions decreases strongly at high temperatures. Also, the irreversibility lines of all the samples irradiated by Pb ions tend to converge at the high-temperature regime of the irreversibility line. This convergence, first observed by Hardy *et al.*,²⁸ provides another indication of the rapid decrease, at high temperatures, of the efficiency of the defects produced by the Pb ions. The surprising observation that the IRL of the Xe sample (B5) decreases more moderately than that of the Pb samples suggests that a new pinning mechanism becomes dominant at high temperatures in the Xe-irradiated sample.

The difference between the irradiation by the Pb and Xe ions can provide an explanation for the above observations. Since the Xe ions produce only clouds of dispersed anisotropic defects, while the Pb ions produce continuous defects, we expect that at low temperatures the Pb irradiation provides more efficient defects. At high temperature, however, vortices start to wander inside and between the clouds. Above some threshold temperature, when the mean amplitude of thermal fluctuations becomes larger than the spacing of clusters within clouds, the defects created by the Xe irradiation become equivalent to columnar defects with the diameter of the clouds.²¹ The efficiency of these columnar de-

fects at high temperatures is higher than those of the columnar defects created by the Pb ions, since the diameter of the clouds seems to be larger. We suggest, therefore, that the origin of the new pinning mechanism in the Xe-irradiated sample is the columnarlike defects created at high temperatures.

C. Density of the pinning force

Figure 4(a) shows F_p as a function of H (we assume that $H \approx B$) for sample B5, irradiated by Xe ions. The data are presented in the normalized coordinates $f_p = F_p/F_{p,\max}$ vs $b^* = H/H_{\max}$, where $F_{p,\max}$ is the maximal value of F_p , and H_{\max} is the value of H at $F_{p,\max}$. The figure demonstrates that below H_{\max} the data for all isotherms below 45 K can be reduced to a single curve. The scaling of the pinning force density for the irradiated samples at temperatures below 45 K indicates that a single dominant pinning mechanism is involved.^{29,30}

The general shape of the curves for $T < 45$ K closely resembles the parabola $f_p(b^*) = b^*(2 - b^*)$. A similar function (though with H_{c2} as the scaling field) has been analytically derived and used for samples with $\Delta\kappa$ pinning of volume defects.³⁰ Different functional forms of $f_p(b^*)$ were recently identified in unirradiated and proton-irradiated $\text{YBa}_2\text{Cu}_3\text{O}_7$ (YBCO) crystals.^{31,32} The difference in the scaling functions is clearly consistent with the difference in the pinning size (point or cloud) taking place in these systems.

The similarity in the functional form of the curves is lost for large fields at $T > 40$ K: the pinning force density does not drop sharply to zero, as is the case for $T < 40$ K, but rather decreases slowly so that a "tail" originates at high fields [see Fig. 4(a)]. For even higher temperatures the scaling in the range $H < H_{\max}$ also breaks down.

A similar scaling was also found in the other irradiated crystals (B1, B2, and B3), at low temperatures. This is demonstrated in Fig. 4(b), which shows f_p vs b^* for the samples B1, B2, and B3 together with B5, at $T = 20$ K. The scaling in the range $H < H_{\max}$ is clearly evident. The general shape of the curves, except for sample B1, follows the function $f_p(b^*) = b^*(2 - b^*)$. At higher temperatures, however, the $f_p(b^*)$ curve develops a tail in the large-field regime, and as the temperature is further increased the scaling in the low-field regime does not hold any more. It is interesting to note that both the unirradiated sample and the sample with the largest dose of irradiation (B4) do not exhibit the scaling discussed above.

The absence of the scaling of the pinning force at temperatures higher than 45 K can possibly be related to the appearance of a tail in the pinning force density curve at high temperatures ($T > 45$ K). A tail in the pinning force density was recently observed in irradiated YBCO crystals,³² and was attributed, using flux creep models, to an increase in the thermal activation. We suggest an alternative explanation, namely that a different pinning mechanism starts to be important for $T > 45$ K. This possibility is consistent with the increase of the critical current of the sample irradiated by Xe ions in comparison to the rapid decrease of the J_c of the samples irradiated by Pb ions, at high temperatures [see Fig. 2(b)].

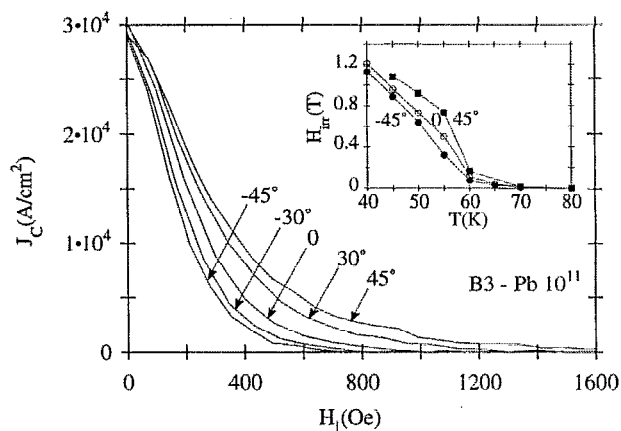


FIG. 5. The critical current density of sample B3, at $T = 60$ K, as a function of H_{\perp} for different field directions. Inset: The irreversible field H_{irr} as a function of temperature for sample B3 for different field directions.

We note that there are several difficulties in our attempt to obtain information from the functional form of $f(b^*)$. First, the scaling holds only up to H_{\max} , and deviations from scaling are observed at high fields. Second, the functional form to which we compare $f(b^*)$ was derived for low-temperature superconductors, for which the scaling field is the upper critical field H_{c2} . Further study is therefore needed in order to establish the relevance of the functional form of $f(b^*)$ to the pinning mechanism in HTS.

D. Angular dependence

The angular dependence of J_c is described in Fig. 5, which shows the critical currents of sample B3 for different angles between the field and the columnar defects. The maximum critical current is obtained for the external field in the direction of the defects (45°), thus demonstrating the unidirectional nature of J_c .

Another demonstration of the unidirectional features is provided in the inset of Fig. 5, which shows the dependence of the irreversibility field on the direction of the field relative to the defect. It is clear that the irreversibility field decreases as the angle between the field and the defect increases. This is a clear indication of the presence of coupling between the layers, which yields the possibility of tilting vortices by an external field; without this coupling the component of the field parallel to the planes penetrates freely and no tilting is possible.^{14,15} At low temperatures, it might be quite difficult to observe unidirectional pinning.¹⁵ However, a closer look reveals angular dependence also in this temperature regime.

E. Relaxation

In this section we present preliminary results on relaxation measurements for Pb-irradiated samples. In these measurements the sample is cooled in the presence of a field of 1.6 T. The field is then turned off and the relaxation is measured. The results should be treated with caution due to the possible effect of self-fields in this procedure. However, the consistency of results of different shapes implies that the effect of self-fields is not dominant. Moreover, we wish to

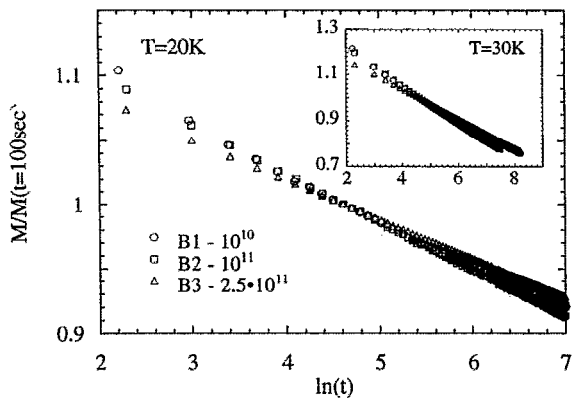


FIG. 6. The magnetic relaxation for the Pb-irradiated samples at $T=20$ K and 30 K (inset). Note: The magnetic moment was divided by its value at $t=100$ sec in order to compare data obtained from different samples.

compare our results to other reports²⁰ in which relaxation at zero field was used. At low temperatures, the relaxation of the irradiated samples in the experimental time window are logarithmic with time. We thus can extract the effective barrier by using $U = kT/(d \ln M/d \ln t)$ and neglect corrections of the interpolation formula. The effective barriers that are extracted from these relaxation rates show a strong decrease as temperature is increased. In Fig. 6 we present the logarithmic relaxation of the remanent magnetization in irradiated samples for 20 and 30 K (inset). It is apparent that at constant temperature the relaxation rates at the various samples are very similar (see an example in Table I), although there are apparent differences in the magnitude of the magnetization. A similar result of converging effective barriers for samples with different irradiation was obtained by Gerhauer *et al.* at $T=10$ K.²⁰ The convergence was interpreted as an indication that the intervortex interactions are not important and thus the effective barrier should reflect only the effective barrier for the depinning of a single vortex from the defect.

In our previous works¹³⁻¹⁵ we reported on apparent unidirectional pinning deduced from the different hysteresis loops for different field directions with respect to the columnar defects. This unidirectional pinning was more apparent above 50 K. At lower temperatures the hysteresis loops look almost identical (see Fig. 1), i.e., the relative anisotropy in $M(H)$ decreases as temperature is decreased. The reduction in the pinning barrier as temperature increases can explain the difference in the relative anisotropy between high and low temperatures. At low temperatures, when the applied field is not in the direction of the defect, the pinning potential is high enough to overcome the Gibbs free energy, and thus the hysteresis loops overlap for various field directions.^{12,15} When the temperature increases the Gibbs energy plays the major role, and unidirectional pinning is observed at all fields.

IV. SUMMARY AND CONCLUSIONS

In this article we have shown that columnar defects created by heavy-ion irradiation can improve the irreversible properties of HTS BSCCO crystals i.e., their J_c , U_{eff} , and

IRL. There is an optimum dose of irradiation (approximately 10^{11} ions/cm²) above which these properties suffer a reduction. Defects produced by Xe ions, although they consist of clouds of clusters, can be treated in the high-temperature range as columnar defects with a diameter defined by the cloud's diameter. We conclude that at the range of temperatures where scaling of the pinning force density holds, a single pinning mechanism (probably $\Delta\kappa$ pinning of volume defects) affects the magnetic behavior. The angular dependence of J_c and IRL leads us to conclude that the vortices in the BSCCO system are linelike vortices. The temperature dependence of U_{eff} can explain the temperature dependence of the relative anisotropy of pinning efficiency of columnar defects.

ACKNOWLEDGMENTS

Extensive collaboration and discussions with M. Konczykowski are acknowledged. The work in Israel is supported by the Ministry of Science and Technology.

- ¹ Y. Yeshurun, A. P. Malozemoff, T. K. Worthington, R. M. Yandroski, L. Krusin-Elbaum, F. H. Holtzberg, T. R. Dinger, and G. V. Chandrashekar, *Cryogenics* **29**, 258 (1989).
- ² J. R. Clem, *Phys. Rev. B* **43**, 7837 (1991).
- ³ J. C. Martinez, S. H. Brongersma, A. Koshelev, B. Ivlev, P. H. Kes, R. P. Griessen, D. G. de Groot, Z. Tarnavski, and A. A. Menovsky, *Phys. Rev. Lett.* **69**, 2276 (1992).
- ⁴ T. Fukami, K. Miyoshi, T. Nishizaki, Y. Horie, F. Ichikawa, and T. Aomine, *Physica C* **202**, 167 (1992).
- ⁵ Y. Iye, S. Nakamura, and T. Tamegai, *Physica C* **159**, 433 (1989).
- ⁶ Y. Iye, I. Oguru, T. Tamegai, W. R. Datars, N. Motohira, and K. Kitazawa, *Physica C* **199**, 154 (1992).
- ⁷ P. H. Kes, J. Aarts, V. M. Vinokur, and C. J. van der Beek, *Phys. Rev. Lett.* **64**, 1063 (1990).
- ⁸ H. Raffy, S. Labdi, O. Laborde, and P. Monceau, *Phys. Rev. Lett.* **66**, 2515 (1991).
- ⁹ S. Martin, A. T. Fiory, R. M. Fleming, G. P. Espinosa, and A. S. Cooper, *Phys. Rev. Lett.* **62**, 677 (1989); *Appl. Phys. Lett.* **54**, 72 (1989).
- ¹⁰ R. Kleiner, F. Steinmeyer, G. Kunkel, and P. Mueller, *Phys. Rev. Lett.* **68**, 2394 (1992).
- ¹¹ M. J. Naughton, R. C. Yu, P. K. Davies, J. E. Fischer, R. V. Chamberlin, Z. Z. Wang, T. W. Jing, N. P. Ong, and P. M. Chaikin, *Phys. Rev. B* **38**, 9280 (1988).
- ¹² J. R. Thompson, Y. R. Sun, H. R. Kerchner, D. K. Christen, B. C. Sales, B. C. Chakoumakos, A. D. Marwick, L. Civale, and J. O. Thompson, *Appl. Phys. Lett.* **60**, 2306 (1992).
- ¹³ L. Klein, E. R. Yacoby, Y. Yeshurun, M. Konczykowski, and K. Kishio, *Physica C* **209**, 251 (1993).
- ¹⁴ L. Klein, E. R. Yacoby, Y. Yeshurun, M. Konczykowski, and K. Kishio, *Physica A* **200**, 413 (1993).
- ¹⁵ L. Klein, E. R. Yacoby, Y. Yeshurun, M. Konczykowski, and K. Kishio, *Phys. Rev. B* **48**, 3523 (1993).
- ¹⁶ V. Hardy, D. Groult, J. Provost, M. Hervieu, B. Raveau, and S. Boffard, *Physica C* **178**, 255 (1991).
- ¹⁷ L. Civale, A. D. Marwick, T. K. Worthington, M. A. Kirk, J. R. Thompson, L. Krusin-Elbaum, Y. Sun, J. R. Clem, and F. Holtzberg, *Phys. Rev. Lett.* **67**, 648 (1991).
- ¹⁸ M. Konczykowski, F. Rullier-Albenque, E. R. Yacoby, A. Shaulov, Y. Yeshurun, and P. Lejay, *Phys. Rev. B* **44**, 7167 (1991).
- ¹⁹ D. Prost, L. Fruchter, I. A. Campbell, N. Motohira, and M. Konczykowski, *Phys. Rev. B* **47**, 3457 (1993).
- ²⁰ W. Gerhauer, G. Ries, H. W. Newmueller, W. Schmidt, O. Eibl, G. Saemann-Ischenko, and S. Klaumunzer, *Phys. Rev. Lett.* **68**, 879 (1992).
- ²¹ M. Konczykowski (private communication).
- ²² N. Motohira, K. Kuwahara, T. Hasegawa, K. Kishio, and K. Kitazawa, *J. Ceram. Soc. Jpn. Int. Ed.* **97**, 994 (1989).
- ²³ C. P. Bean, *Phys. Rev. Lett.* **8**, 250 (1962); *Rev. Mod. Phys.* **36**, 31 (1964).
- ²⁴ A. M. Campbell and J. E. Evetts, *Adv. Phys.* **21**, 199 (1972).
- ²⁵ M. Daumling and D. C. Larbalestier, *Phys. Rev. B* **40**, 9350 (1989).

- ²⁶D. R. Nelson and V. M. Vinokur, *Phys. Rev. Lett.* **68**, 2398 (1992).
- ²⁷M. Konczykowski, N. Chikumoto, V. M. Vinokur, and M. Feigel'man (unpublished).
- ²⁸V. Hardy, Ch. Simon, J. Provost, and D. Groult, *Physica C* **205**, 371 (1993).
- ²⁹A. M. Campbell and J. E. Evetts, *Critical Currents in Superconductors* (Taylor & Francis, London, 1972), Chaps. 7 and 8; H. Ullmaier, *Irreversible Properties of Type II Superconductors* (Springer, Berlin, 1975), Chaps. 3–5.
- ³⁰D. Dew-Hughes, *Philos. Mag.* **30**, 293 (1974).
- ³¹L. Klein, E. R. Yacoby, Y. Yeshurun, A. Erb, G. Müller-Vogt, U. Breit, and H. Wühl, *Phys. Rev. B* (to be published).
- ³²L. Civale, M. W. McElfresh, A. D. Marwick, F. Holtzberg, C. Feild, J. R. Thompson, and D. K. Christen, *Phys. Rev. B* **43**, 13732 (1991).